




Kinetic, equilibrium, and thermodynamic performance of sulfonamides adsorption onto graphene

Shuting Zhuang¹ · Xin Zhu² · Jianlong Wang^{1,3} 

Received: 13 April 2018 / Accepted: 27 September 2018 / Published online: 30 October 2018
© Springer-Verlag GmbH Germany, part of Springer Nature 2018

Abstract

With the extensive production and consumption of sulfonamide antibiotics, their existence in aquatic environments has received increasing attention due to their acute and chronic toxic effects. In this study, graphene was characterized and applied for sulfamethazine (SMT) removal from aqueous solution. The effect of the contact time (0–1440 min), initial concentration (2–100 mg L⁻¹), and temperature (298–318 K), as well as pH (2–9) and ionic strength (0–0.2 M NaNO₃), have been examined. The maximum adsorption capacity was calculated to be 104.9 mg g⁻¹ using the Langmuir model. The endothermic adsorption process ($\Delta H = 10.940$ kJ mol⁻¹) was pH- and temperature-dependent, and the adsorption data fitted well with the Langmuir isothermal and the pseudo second-order kinetic models. Additionally, ionic strength (0.01 to 0.2 M NaNO₃) had no obvious influence on SMT adsorption by graphene. Ultimately, graphene proved to be an effective adsorbent for sulfonamide antibiotics removal from aqueous solutions.

Keywords Graphene · Antibiotics · Sulfamethazine · Adsorption · Kinetics

Introduction

Sulfonamides (SAs) is a general term that describes a class of drugs with the structure of sulfanilamide. It has been extensively used in chemical therapy for the prevention and treatment of bacterial infectious diseases (Aminov 2017). In spite of its extraordinary antibacterial effect, there are concerns over the drug abuse, which may result in super bacteria and efficacy failure. However, its extensive application in livestock production accompanied by substantial unabsorbed SAs discharging to waters has aroused much attention. As the biggest producer and user of SAs, China is in great potential risks of this pollution, for more and more SAs have been detected in

the environments (Bu et al. 2013; Gao et al. 2016; Zhao et al. 2016; Chen et al. 2017; Ren et al. 2018; Wang et al. 2019). Concerns arising from exposure to sulfonamide antibiotics in aquatic environments, which may lead to toxic effects and microorganism antibiotic resistance, have stimulated the development of its removal technology. It is of great significance to develop an effective and economical technology to remove the SA residue from water (Wang and Wang 2016).

Various technologies have been studied for the removal of antibiotics from water and wastewater, including physical, chemical, and biological methods, which have the potential to remove pathogens, antibiotic resistance genes (ARG), and emerging contaminants in an environmental and economical manner (Pang et al. 2016; Wang and Chu 2016; Ducey et al. 2017; Liu et al. 2017a, b, 2018; Song et al. 2017; Tang and Wang 2018; Wang and Wang 2018a). A series of technologies have been developed for SA removal, such as adsorption and advanced oxidation processes (AOPs) (Homem and Santos 2011; Wang and Bai 2017). Compared with physical and chemical methods, the biological treatment (e.g., activated sludge method) has been recognized as the most economical and effective one for most organic pollutants (Wang and Wang 2018b). Whereas, there is a controversy over the potential cultivation of resistance gene and spread risks. Previously,

Responsible editor: Philippe Garrigues

✉ Jianlong Wang
wangjl@tsinghua.edu.cn

¹ Collaborative Innovation Center for Advanced Nuclear Energy Technology, INET, Tsinghua University, Beijing 100084, People's Republic of China

² China Three Gorges Projects Development Co., Ltd, Chengdu 610041, People's Republic of China

³ Beijing Key Laboratory of Radioactive Waste Treatment, INET, Tsinghua University, Beijing 100084, People's Republic of China

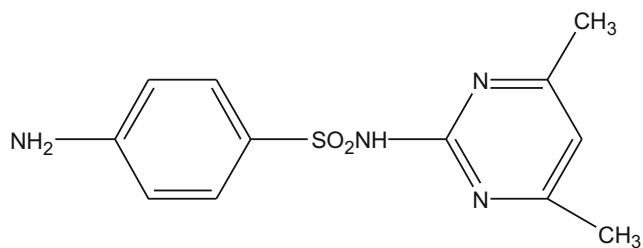


Fig. 1 Chemical structure of SMT

our research group has conducted a series of studies on AOPs for SMA degradation, including Fenton-like reaction (Wan et al. 2016; Bai et al. 2017; Wan and Wang 2017a, b), and gamma irradiation (Liu and Wang 2013; Liu et al. 2014; Chu et al. 2015). Although known for its degradation capacity, AOPs suffer from its relatively high cost. Among all these methods, adsorption has been extensively studied due to its ease of operation, as well as the overcoming of these above discussed disadvantages (Chi et al. 2017; Wang et al. 2018).

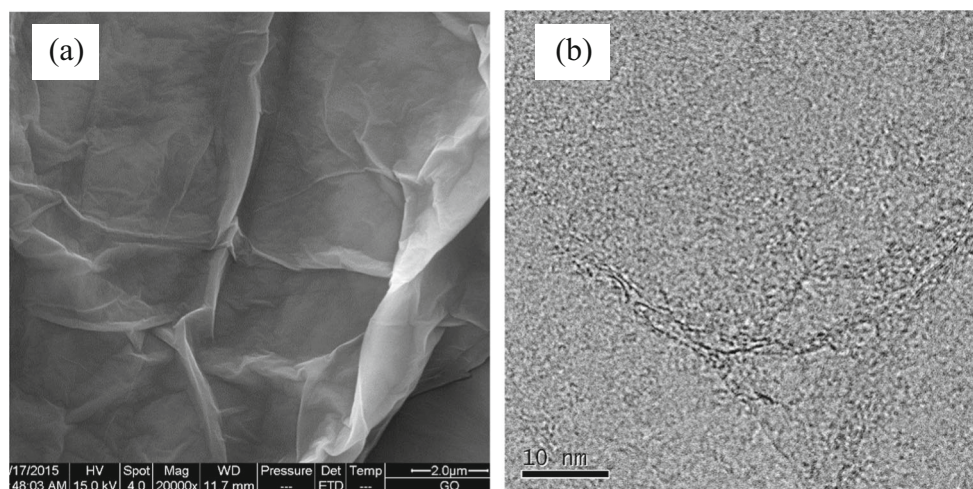
Various kinds of adsorbents have been used for SA removal (Zhang et al. 2016), such as resin, organophilic zeolite Y, carbon-based adsorbents, and metal-organic frameworks (MOF). Although MOF exhibited a potential for sulfamethazine (SMT) removal, its cost is still too high (Azhar et al. 2017). As for resin, its removal efficiency for SMT is still not yet satisfactory and its adsorption process is pH- or ionic strength-dependent (Yang et al. 2011). The adsorption of sulfonamides onto organophilic zeolite Y was irreversible, which is not favorable for regeneration (Braschi et al. 2010). Among these adsorbents, carbon-based adsorbent is one category that is economical and easy to be obtained (Xu and Wang 2017). There have been lots of researches on the application of activated carbon for water purification, including the removal of SAs (Choi et al. 2008; Nam et al. 2014; Liu et al. 2017a, b). Considering the uniform and high surface area of the structure,

the other carbon-based material, graphene, is regarded as an alternative adsorbent for the removal of SAs.

As a two-dimensional honeycomb-like material, graphene is composed of carbon atoms that covalently connect each other via sp^2 hybrid orbitals (Allen et al. 2010). This unique structure enriches itself with a high surface area and high surface hydrophobicity, which is good for adsorption. The application of graphene family for organic compound adsorption (e.g., antibiotics) has been well summarized by Perreault et al. (2015). Previously, the adsorption of bisphenol A and triclosan into graphene has been studied by the comparison of using activated carbon. The results showed that graphene was superior to activated carbon for triclosan adsorption, but not for bisphenol A (Wang et al. 2017). Rostamian and Behnejad (2018) utilized graphene nanosheet as an effective adsorbent for doxycycline removal. A maximum adsorption capacity of 110 mg g^{-1} was achieved according to the Hill equation. Furthermore, Das et al. (2017) found that π - π and hydrophobic forces were mainly responsible for adsorption using pristine graphene. These previous studies using graphene for various antibiotics indicate great potential of graphene as an adsorbent for SAs removal. However, there is a lack of related knowledge. The fundamental study of SAs into the pristine graphene can provide further insight into adsorption performance, which is good for future modification and application.

In this study, sulfamethazine (SMT), which belongs to SAs, was chosen as target pollutant. Its structure is shown in Fig. 1. We intended to investigate the performance of SMT adsorption onto graphene. The physicochemical and morphological properties of graphene were studied using SEM, BET, and zeta potential measuring equipment. The effect of contacting time, adsorbent dosage, temperature, pH, and ionic strength on SMT adsorption was also investigated.

Fig. 2 SEM (a) and TEM (b) images of graphene



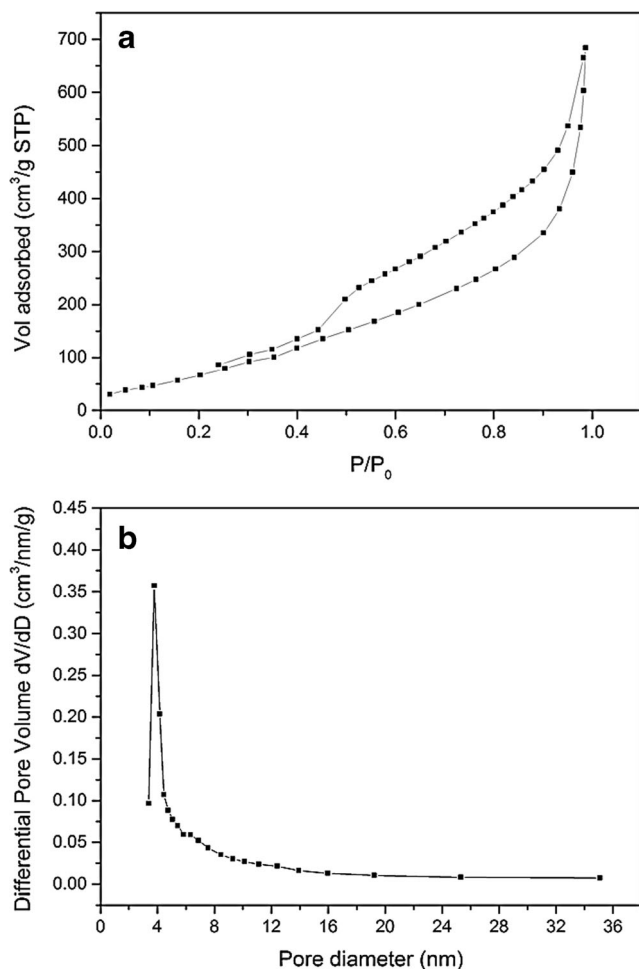


Fig. 3 N₂ sorption/desorption isotherms (a) and pore size distribution curves (b) of graphene

Materials and methods

Chemicals

The graphene was obtained from The Sixth Element (Changzhou) Materials Technology Co., Ltd. (China). SMT was obtained from the Thermo Fisher Scientific Inc. (America). The other chemical reagents of analytical grade were purchased from Sinopharm Chemical Reagent Co., Ltd. (China). Meanwhile, all solutions were prepared with deionized water without further purification.

Table 1 Physical property of the graphene

S _A BET (m ² g ⁻¹)	Mesopore (cm ³ g ⁻¹)	Average pore size (nm)
271.10	1.13	3.78

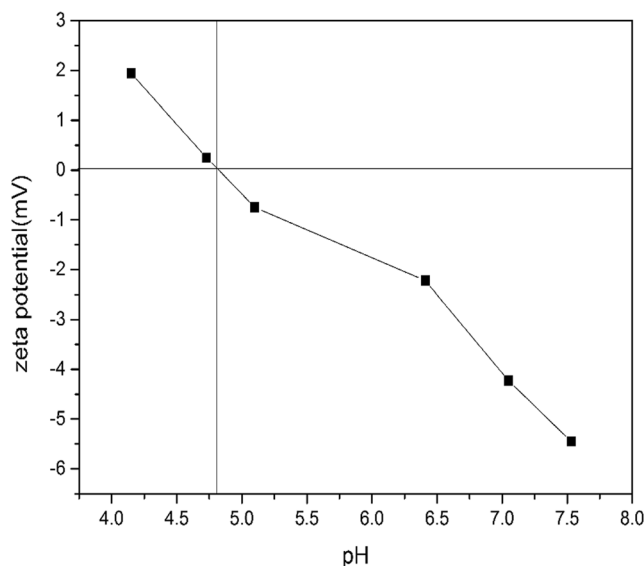


Fig. 4 Zeta potential curves vs. pH of graphene

Characterization of adsorbents

The morphologies of graphene were characterized by a field emission scanning electron microscope (Hitachi SU-8010) and high-resolution transmission electron microscope (JEM-2010). The Brunauer–Emmett–Teller (BET) surface area was examined by nitrogen sorption/desorption isotherm measurements at 77 K on a NOVA 3200e surface area and porosity analyzer. The zeta potential of graphene in aqueous solution was determined by zeta potential measuring instrument (JS94H₂, Powereach, Shanghai).

Adsorption experiments

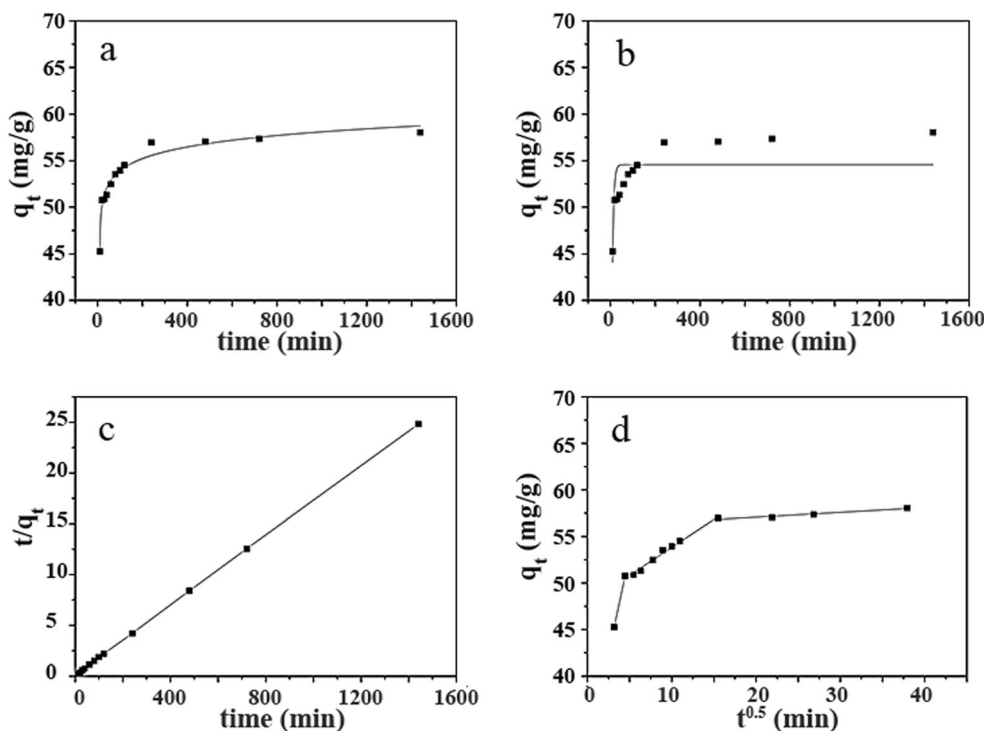
SMT adsorption experiments were performed in a batch system. Graphene was added into 25-mL conical flasks which contained SMT solutions. The pH value was adjusted with 0.1 M HCl or 0.1 M NaOH, and the ionic strength of solution was adjusted by NaNO₃. Besides, the conical flasks were all shaken in a water-bath shaker at 150 rpm and room temperature (about 25 °C). The other conditions were given in the figure legends.

The adsorption capacity of the adsorbent was calculated according to the following equation:

$$q_t = \left(\frac{C_0 - C_t}{m} \right) V$$

where C_0 is the initial SMT concentration, C_t is the concentration of SMT at time t , m is the mass of the adsorbent, and V is the volume of the solution.

Fig. 5 Sorption kinetics of SMT by graphene. Conditions: $V = 10$ mL, $C_0 = 20$ mg/L, $I = 0.02$ M NaNO_3 , $\text{pH} = 7$, dosage = 0.2 g/L, $T = 298$ K, and $r = 150$ rpm



Analytical methods

SMT concentrations were quantified by high-performance liquid chromatograph (HPLC) (Agilent 1200 Series, Agilent, USA) equipped with a diode array detector (DAD) and an XDB-C18 (4.6×150 mm) column. The detection wavelength was 255 nm and the column temperature was 30 °C. The mobile phase was a mixture of distilled water and ethanol in a ratio of 55:45 (v/v).

Results and discussion

Characterization of sorbents

The morphologies of graphene were shown in Fig. 2. There were typical ripples on its surfaces. Graphene nanosheet films were transparent and slightly aggregated with the wrinkles loosely distributed on the basal planes forming groove regions. The potential adsorption sites could be divided into flat surfaces and groove regions.

The N_2 sorption/desorption isotherms, as well as the pore size-distribution curves of graphene, were presented in Fig. 3. According to the Brunauer–Deming–Deming–Teller (BDDT) classification, the isotherms and hysteresis loops were type IV and type H3, respectively (Zhu and Wang 2017). This indicated that the pore size was relatively uniform and the pores were mesoporous ($1.126 \text{ cm}^3 \text{ g}^{-1}$), as confirmed by the corresponding pore size-distribution curves. The feature analysis data, as presented in Table 1, showed that the average pore size was 3.78 nm. While the specific surface area was $271.10 \text{ m}^2 \text{ g}^{-1}$, which was lower than the theoretical value ($2600 \text{ m}^2 \text{ g}^{-1}$) (Park and Ruoff 2009) due to the blending and curling of the graphene sheets.

Zeta potential is the potential difference between the dispersion medium and the stationary layer of fluid attached to the dispersed particle, which can express the acidity or basicity of the sorbent surfaces (Xing et al. 2016). The variation of the zeta potentials of graphene samples with pH was presented in Fig. 4, indicating that zeta potential gradually changed from positive to negative as the increase of pH values. While the surface charges of the samples changed from positive to negative at the same time. In neutral

Table 2 Kinetics parameters for SMT adsorption by graphene

Pseudo first-order				Pseudo second-order			
k_1 (min^{-1})	$q_{e(\text{cal})}$ (mg g^{-1})	$q_{e(\text{exp})}$ (mg g^{-1})	R^2	k_2 ($\text{g mg}^{-1} \text{ min}^{-1}$)	$q_{e(\text{cal})}$ (mg g^{-1})	k ($\text{mg g}^{-1} \text{ min}^{-1}$)	R^2
0.165	–	58.05	0.534	2.953×10^{-3}	58.14	9.98	> 0.999

Table 3 Parameters of intraparticle diffusion model for SMT adsorption by graphene

Phase	C (mg g ⁻¹)	k_{WM} (mg g ⁻¹ min ^{-0.5})	R^2
1	31.97	4.199	–
2		0.599	0.985
3		0.051	0.930

condition, graphene, with negative charge, was more likely to adsorb cationic molecules, which was suitable for SMT adsorption in this study. Additionally, the potential of zero charge (pH_{PZC}) of graphene was 4.83, indicating the existence of substantial acidic functional groups on its surface (Ding et al. 2013).

Effect of contact time on SMT adsorption

The absorption kinetic curve of SMT onto graphene was shown in Fig. 5a. At first, owing to the abundant unoccupied adsorption sites, as well as the high concentration gradient (Zhuang et al. 2017), the adsorption of SMT onto graphene was very fast within the first 10 min. Then, the adsorption amount plateaued and reached its maximum in 4 h with an adsorption capacity of 58.05 mg g⁻¹.

To investigate the kinetic sorption mechanism and the rate-limiting step during the process, the pseudo first-order, pseudo second-order, and Weber–Morris models were adopted to analyze the effect of contact time on the adsorption of SMT, and the corresponding curves were shown in Fig. 5b–d.

The pseudo first-order equation can be expressed as

$$\log(q_e - q_t) = \log q_e - k_1 t \quad \ln(q_e - q_t) = \ln q_e - k_1 t \tag{1}$$

where q_e and q_t are the amount of SMT adsorbed at equilibrium and time t , respectively, and k_1 is the rate constant.

The pseudo second-order equation can be described as

$$\frac{t}{q} = \frac{1}{k_2 q_e^2} + \frac{t}{q_e} \tag{2}$$

where k_2 is the rate constant of the pseudo second-order equation.

The related parameters were calculated and presented in Table 2. The correlation coefficient (R^2) of the pseudo first- and pseudo second-order equations was 0.534 and > 0.999, respectively. In addition, the calculated adsorption capacity ($q_{e(cal)} = 58.14 \text{ mg g}^{-1}$) obtained from the pseudo second-order equation was very close to the experimental one ($q_{e(exp)} = 58.05 \text{ mg g}^{-1}$), which indicated that the pseudo second-order kinetic model was more suitable to this adsorption process (Zhuang et al. 2018). While this adsorption process was assumed to be chemical sorption (Ho and McKay 1999).

The Weber–Morris equation can be expressed as

$$q_t = k_{WM} t^{1/2} + C \tag{3}$$

where C is the constant that involves thickness and boundary layer, and k_{WM} is the constant of the intraparticle diffusion model.

The application of this model for data fitting was presented in Fig. 5d and its parameters were shown in Table 3. The whole adsorption process could be divided into three processes, including the surface adsorption, channel slow diffusion, and equilibrium. As the curves did not go through the origin, it was induced that the intraparticle diffusion was not the only rate-limiting step during the adsorption process. Meanwhile, the intercept (C) was positive value, revealing that intraparticle diffusion was not disturbed by boundary layer.

Adsorption isotherms and thermodynamics of SMT

Combining with the characteristics of the data of the present study, the Langmuir, Freundlich, Henry, and Temkin isothermal models were used to fit the sorption isotherm and sorption process was studied through the parameters obtained by the fitting curves. The linear relation formulas of these four models are as follows (Wang and Zhuang 2017):

$$\text{Langmuir equation : } \frac{C_e}{q_e} = \frac{C_e}{q_{max}} + \frac{1}{k_L q_{max}} \tag{4}$$

$$\text{Freundlich equation : } \ln q_e = \ln k_F + n \ln C_e \tag{5}$$

$$\text{Henry equation : } q_e = k_H C_e \tag{6}$$

$$\text{Temkin equation : } q_e = k_T \ln C_e + k_T \ln f \tag{7}$$

where C_e is the concentration of SMT at equilibrium, q_e is the amount of SMT adsorbed at equilibrium, and q_{max} (mg g⁻¹) is the theoretical maximum sorption capacity per unit weight of adsorbent. k_L , k_F , k_H , and k_T are sorption constants of the

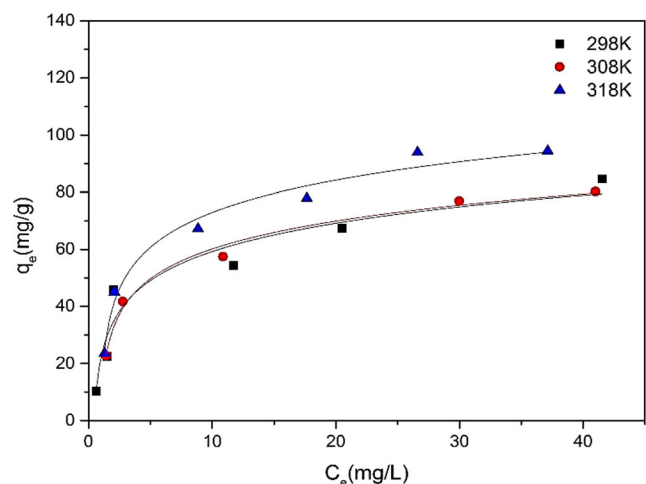


Fig. 6 Sorption isotherms of SMT by graphene at 298, 308, and 318 K. Other conditions: $V = 10 \text{ mL}$, $C_0 = 2\text{--}100 \text{ mg/L}$, $I = 0.02 \text{ M NaNO}_3$, $\text{pH} = 7$, dosage = 0.2 g/L, and $r = 150 \text{ rpm}$

Table 4 Isotherm parameters for adsorption of SMT by graphene

Temperature (K)	Langmuir			Freundlich			Henry		Temkin	
	q_{\max} (mg g ⁻¹)	k_L (L mg ⁻¹)	R^2	k_F	n	R^2	k_H (L g ⁻¹)	R^2	k_T	R^2
298	91.08	0.201	0.969	26.491	0.311	0.744	2.471	0.768	14.998	0.842
308	87.79	0.238	0.996	24.028	0.343	0.901	2.353	0.796	16.438	0.977
318	104.93	0.234	0.991	27.110	0.372	0.890	3.262	0.826	20.180	0.968

Langmuir, Freundlich, Henry, and Temkin models, respectively.

The sorption isotherms of SMT were shown in Fig. 6 and the fitting results of these models were shown in Table 4. As shown in Fig. 6 and Table 4, the adsorption capacity of SMT at equilibrium increased with increasing SMT concentration and reached equilibration progressively. The maximum adsorption capacity was approximately 104.93 mg g⁻¹ at 318 K. In the scope of measured concentration, only the Langmuir model fitted all experimental data very well ($R^2 > 0.97$), indicating a monolayer adsorption process (Xu and Wang 2017). In addition, the Temkin model fitted reasonably, implicating the importance of electrostatic interaction in this process. Although the correlation coefficients (R^2) of the Freundlich model varied significantly at different temperatures, the fact that values of n were all between 0.1 and 0.5 can still illustrate that the adsorbent had high sorption capacity and the distribution of sorption energy was highly heterogeneous.

The relation of standard Gibbs free energy change and standard equilibrium constant under standard state is as follows:

$$\Delta G = -RT \ln k_H \quad (8)$$

where R (8.314 J mol⁻¹ K⁻¹) is gas constant, T is absolute temperature, and k_H is equilibrium sorption constant of the Henry model.

Sorption enthalpy is associated with van der Waals force between adsorbate and sorbent. While the sorption entropy measures the freedom of adsorbate molecules. The formula including Gibbs free energy change quantity, enthalpy change, and entropy change can be calculated according to following equation

$$\Delta G = \Delta H - T\Delta S \quad (9)$$

Combining Eqs. (8) and (9), it can be inferred that:

$$\ln k_H = \frac{-\Delta G}{RT} = \frac{-\Delta H}{RT} + \frac{\Delta S}{R} \quad (10)$$

The value of k_H in Table 4 was substituted into the above equation to calculate the free energy change (ΔG), enthalpy change (ΔH), and entropy change (ΔS), and the results were listed in Table 5. The values of ΔH (10.94 kJ mol⁻¹) were significantly larger than zero, illustrating that the sorption was endothermic process. Besides, ΔS (0.44 kJ mol⁻¹ K⁻¹) was greater than zero, revealing that the contribution of

entropy change in sorption course for free energy quantity cannot be ignored. At the given temperature (298–318 K), the ΔG was less than zero, indicating that the adsorption of SMT on graphene is a spontaneous process.

Effect of pH on SMT adsorption

The value of solution pH plays an important role in the adsorption process, involving not only the species of adsorbates but also the surface charge state of the adsorbent. The effect of pH on the adsorption of SMT was studied and presented in Fig. 7. Results showed that the optimal pH was between 5 and 8, and neutral condition (pH = 7) exhibited highest adsorption capacity for SMT according to the given data. Higher or lower pH would result in lower adsorption capacity, which indicated that electrostatic interaction may dominate the adsorption process. For the adsorbates, the pK_{a1} of SMT were 2.28 (pK_{a1}) and 7.42 (pK_{a2}), suggesting that there are zwitterionic species when pH was in the range of 2.28–7.42, positively charged species when pH < 2.28 and negatively charged species when pH > 7.42 (Kurwadkar et al. 2007).

When pH > 7.42, negatively charged species of SMT dominated in solution, while the surface of graphene was also negatively charged (pH_{PZC} = 4.83). The electrostatic repulsion between the adsorbent and adsorbate of the same negative charges may account for the suppressed sorption. On the other hand, at lower pH, SMT mainly presented in neutral form at pH 2.28–7.42, but there are also other small portion of cationic and anionic forms. At the optimal pH range (5–8), the adsorbents were positively charged, leading to the electrostatic attraction for anionic SMT, but electrostatic repulsion for cationic SMT, as shown in Fig. 8. Additionally, there were electrostatic interactions between the zwitterionic SMT and adsorbents. Furthermore, the hydrophobic property of protonation of zwitterionic SMT was stronger than deprotonation of

Table 5 Thermodynamic parameters for SMT sorption by graphene

Temperature (K)	ΔG (kJ mol ⁻¹)	ΔH (kJ mol ⁻¹)	ΔS (kJ mol ⁻¹ K ⁻¹)
298	-2.241	10.94	0.44
308	-2.191		
318	-3.126		

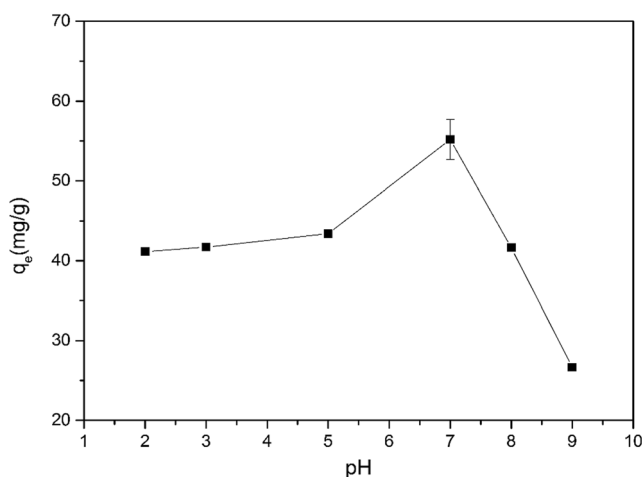


Fig. 7 Effect of pH on the equilibrium sorption capacity of SMT by graphene. Conditions: $V = 10$ mL, $C_0 = 20$ mg/L, $I = 0.02$ M NaNO_3 , $\text{pH} = 2-9$, dosage = 0.2 g/L, $T = 298$ K, and $r = 150$ rpm

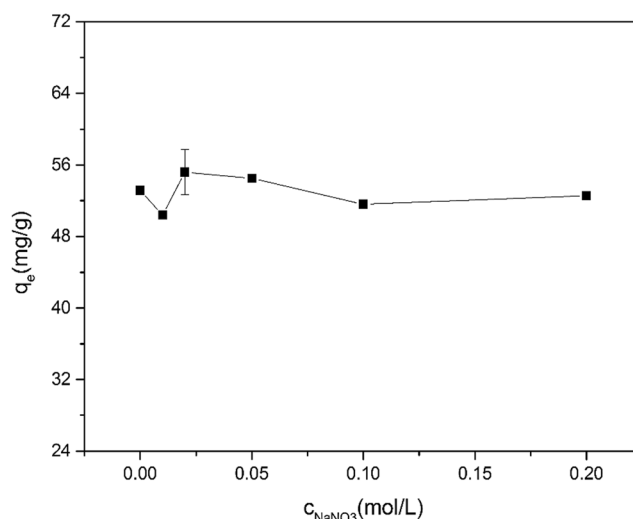


Fig. 9 Effect of ionic strength on the equilibrium sorption capacity of SMT by graphene. Conditions: $V = 10$ mL, $C_0 = 20$ mg/L, $I = 0.01-0.2$ M NaNO_3 , $\text{pH} = 7$, dosage = 0.2 g/L, $T = 298$ K, and $r = 150$ rpm

anionic SMT. The increase of neutral SMT for attracting π electron will lead to strengthening of π - π EDA interaction between the deionization group and graphene carbon structure with π electron (Lertpaitoonpan et al. 2009).

Effect of ionic strength on SMT adsorption

To study the effect of ionic strength, the adsorption of SMT experiments were conducted with the electrolyte, NaNO_3 ,

ranging from 0 to 0.2 mol L⁻¹. These ions (Na^+ and NO_3^-) may affect SMT adsorption by competing with SMT for adsorption sites or creating general effect of “ionic atmosphere” or saline effect” (Radovic et al. 2001). However, as shown in Fig. 9, ionic strength did not have obvious effect on SMT adsorption. This phenomena clearly indicated that the added ions did not compete with SMT for adsorption sites, and the electrostatic shielding effect did not affect adsorption capacity obviously.

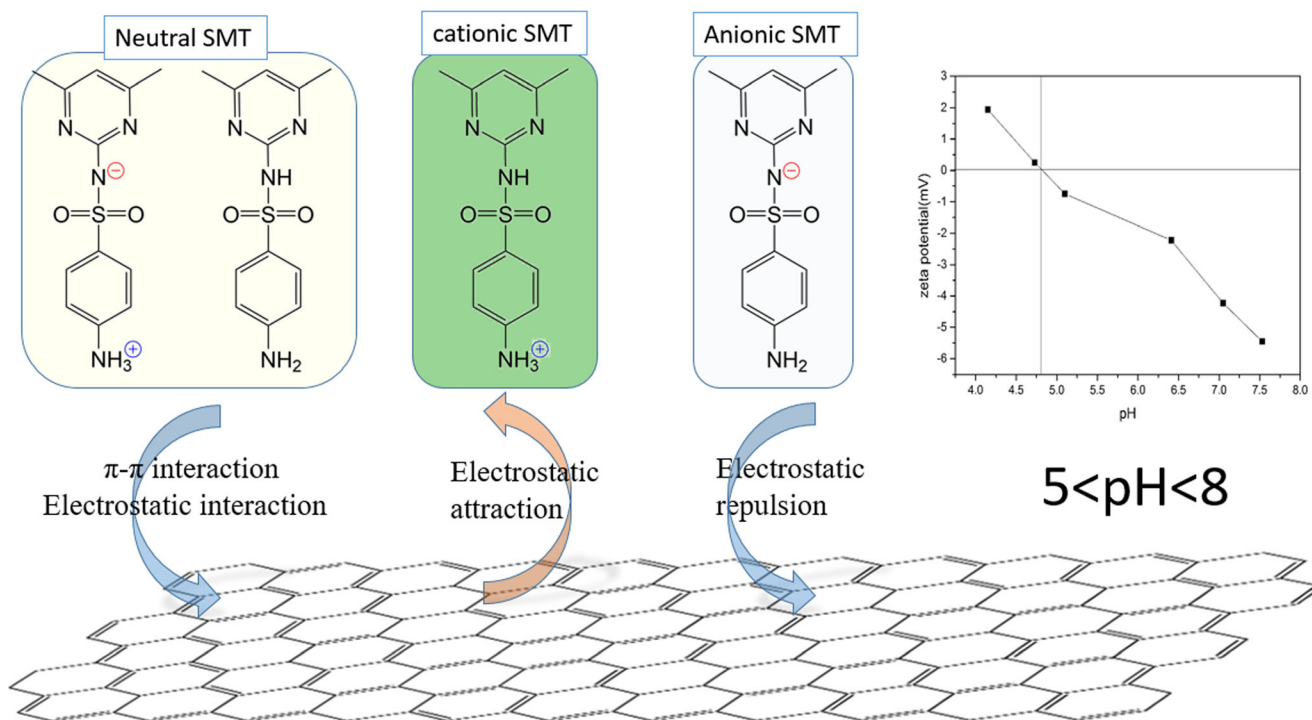


Fig. 8 The proposed adsorption mechanism of SMT onto graphene at pH 5–8

Conclusions

Graphene was favorable for adsorbing SMT from aqueous solution. With a high specific surface area ($271.10 \text{ m}^2 \text{ g}^{-1}$) and a low pH_{PZC} (4.83), graphene could adsorb SMT with a capacity of 104.9 mg g^{-1} . This adsorption process was greatly influenced by solution pH and temperature, and less affected by ionic strength. Neutral pH condition was more suitable for SMT adsorption due to the charge states of the adsorbates and adsorbents, as well as the π - π interaction. The measured data of the kinetic and equilibrium experiments fitted well with the pseudo second-order kinetic and the Langmuir isothermal models. According to the thermodynamics, ΔH and ΔS was calculated to be $10.94 \text{ kJ mol}^{-1}$ and $0.44 \text{ kJ mol}^{-1} \text{ K}^{-1}$, respectively. The findings in this study highlight graphene as a potential adsorbent for the removal of SMT from aqueous solution.

Funding The research was supported by the National Natural Science Foundation of China (51338005) and the Program for Changjiang Scholars and Innovative Research Team in College (IRT-13026).

References

- Allen MJ, Tung VC, Kaner RB (2010) Honeycomb carbon: a review of graphene. *Chem Rev* 110:132–145
- Aminov R (2017) History of antimicrobial drug discovery: major classes and health impact. *Biochem Pharmacol* 133:4–19
- Azhar MR, Abid HR, Periasamy V, Sun HQ, Tade MO (2017) Adsorptive removal of antibiotic sulfonamide by UiO-66 and ZIF-67 for wastewater treatment. *J Colloid Interface Sci* 500:88–95
- Bai ZY, Yang Q, Wang JL (2017) Degradation of sulfamethazine antibiotics in Fenton-like system using Fe_3O_4 magnetic nanoparticles as catalyst. *Environ Prog Sustain Energy* 36:1743–1753
- Braschi I, Blasioli S, Gigli L, Gessa CE, Alberti A, Martucci A (2010) Removal of sulfonamide antibiotics from water: evidence of adsorption into an organophilic zeolite Y by its structural modifications. *J Hazard Mater* 178:218–225
- Bu QW, Wang B, Huang J, Deng SB, Yu G (2013) Pharmaceuticals and personal care products in the aquatic environment in China: a review. *J Hazard Mater* 262:189–211
- Chen CQ, Zheng L, Zhou JL, Zhao H (2017) Persistence and risk of antibiotic residues and antibiotic resistance genes in major mariculture sites in Southeast China. *Sci Total Environ* 580:1175–1184
- Chi T, Zuo JN, Liu FL (2017) Performance and mechanism for cadmium and lead adsorption from water and soil by corn straw biochar. *Front Environ Sci Eng* 11:15
- Choi KJ, Kim SG, Kim SH (2008) Removal of tetracycline and sulfonamide classes of antibiotic compound by powdered activated carbon. *Environ Technol* 29:333–342
- Chu LB, Wang JL, Liu YK (2015) Degradation of sulfamethazine in sewage sludge mixture by gamma irradiation. *Radiat Phys Chem* 108:102–105
- Das R, Vecitis CD, Schulze A, Cao B, Ismail AF, Lu X, Chen J, Ramakrishna S (2017) Recent advances in nanomaterials for water protection and monitoring. *Chem Soc Rev* 46(22):6946–7020
- Ding D, Lei Z, Yang Y, Feng C, Zhang Z (2013) Nickel oxide grafted andic soil for efficient cesium removal from aqueous solution: adsorption behavior and mechanisms. *ACS Appl Mater Interfaces* 5:10151–10158
- Ducey TF, Collins JC, Ro KS, Woodbury BL, Griffin DD (2017) Hydrothermal carbonization of livestock mortality for the reduction of pathogens and microbially-derived DNA. *Front Environ Sci Eng* 11(3): DOI: <https://doi.org/10.1007/s11783-017-0930-x>
- Gao J, Huang J, Chen WW, Wang B, Wang YJ, Deng SB, Yu G (2016) Fate and removal of typical pharmaceutical and personal care products in a wastewater treatment plant from Beijing: a mass balance study. *Front Environ Sci Eng* 10:491–501
- Ho YS, McKay G (1999) Pseudo-second order model for sorption processes. *Process Biochem* 34:451–465
- Homem V, Santos L (2011) Degradation and removal methods of antibiotics from aqueous matrices—a review. *J Environ Manag* 92:2304–2347
- Kurwadkar ST, Adams CD, Meyer MT, Kolpin DW (2007) Effects of sorbate speciation on sorption of selected sulfonamides in three loamy soils. *J Agric Food Chem* 55:1370–1376
- Lertpaitoonpan P, Ong SK, Moorman TB (2009) Effect of organic carbon and pH on soil sorption of sulfamethazine. *Chemosphere* 76:558–564
- Liu Y, Fan Q, Wang JL (2018) Zn-Fe-CNTs catalytic in situ generation of H_2O_2 for Fenton-like degradation of sulfamethoxazole. *J Hazard Mater* 342:166–176
- Liu YK, Hu J, Wang JL (2014) Fe^{2+} enhancing sulfamethazine degradation in aqueous solution by gamma irradiation. *Radiat Phys Chem* 96:81–87
- Liu QQ, Li M, Zhang FW, Yu HC, Zhang Q, Liu X, (2017a) The removal of trimethoprim and sulfamethoxazole by a high infiltration rate artificial composite soil treatment system. *Front Environ Sci Eng* 11(2). <https://doi.org/10.1007/s11783-017-0920-z>
- Liu Y, Liu XH, Dong WP, Zhang LL, Kong Q, Wang WL (2017b) Efficient adsorption of sulfamethazine onto modified activated carbon: a plausible adsorption mechanism. *Sci Rep* 7:12437
- Liu YK, Wang JL (2013) Degradation of sulfamethazine by gamma irradiation in the presence of hydrogen peroxide. *J Hazard Mater* 250:99–105
- Nam SW, Choi DJ, Kim SK, Her N, Zoh KD (2014) Adsorption characteristics of selected hydrophilic and hydrophobic micropollutants in water using activated carbon. *J Hazard Mater* 270:144–152
- Pang YC, Huang JJ, Xi JY, Hu HY, Zhu Y (2016) Effect of ultraviolet irradiation and chlorination on ampicillin-resistant *Escherichia coli* and its ampicillin resistance gene. *Front Environ Sci Eng* 10:522–530
- Park S, Ruoff RS (2009) Chemical methods for the production of graphenes. *Nat Nanotechnol* 4(4):217–224
- Perreault F, Fonseca de Faria A, Elimelech M (2015) Environmental applications of graphene-based nanomaterials. *Chem Soc Rev* 44(16):5861–5896
- Radovic LR, Moreno-Castilla C, Rivera-Utrilla J (2001) Carbon materials as adsorbents in aqueous solutions. *Chem Phys Carbon* 27:227–405
- Ren X, Zeng G, Tang L, Wang J, Wan J, Liu Y, Yu J, Yi H, Ye S, Deng R (2018) Sorption, transport and biodegradation—an insight into bioavailability of persistent organic pollutants in soil. *Sci Total Environ* 610-611:1154–1163
- Rostamian R, Behnejad H (2018) Insights into doxycycline adsorption onto graphene nanosheet: a combined quantum mechanics, thermodynamics, and kinetic study. *Environ Sci Pollut Res* 25: 2528–2537
- Song XY, Liu R, Chen LJ, Kawagishi T (2017) Comparative experiment on treating digested piggery wastewater with a biofilm MBR and conventional MBR: simultaneous removal of nitrogen and antibiotics. *Front Environ Sci Eng* 11(2). <https://doi.org/10.1007/s11783-017-0919-5>
- Tang JT, Wang JL (2018) Metal organic framework with coordinatively unsaturated sites as efficient Fenton-like catalyst for enhanced degradation of sulfamethazine. *Environ Sci Technol* 52:5367–5377

- Wan Z, Hu J, Wang JL (2016) Removal of sulfamethazine antibiotics using Ce-Fe-graphene nanocomposite as catalyst by Fenton-like process. *J Environ Manag* 182:284–291
- Wan Z, Wang JL (2017a) Degradation of sulfamethazine using Fe₃O₄-Mn₃O₄/reduced graphene oxide hybrid as Fenton-like catalyst. *J Hazard Mater* 324:653–664
- Wan Z, Wang JL (2017b) Fenton-like degradation of sulfamethazine using Fe₃O₄/Mn₃O₄ nanocomposite catalyst: kinetics and catalytic mechanism. *Environ Sci Pollut Res* 24:568–577
- Wang JL, Bai ZY (2017) Fe-based catalysts for heterogeneous catalytic ozonation of emerging contaminants in water and wastewater. *Chem Eng J* 312:79–98
- Wang JL, Chu LB (2016) Irradiation treatment of pharmaceutical and personal care products (PPCPs) in water and wastewater: an overview. *Radiat Phys Chem* 125:56–64
- Wang F, Lu X, Peng W, Deng Y, Zhang T, Hu Y, Li XY (2017) Sorption behavior of bisphenol a and triclosan by graphene: comparison with activated carbon. *ACS Omega* 2(9):5378–5384
- Wang JL, Wang SZ (2016) Removal of pharmaceuticals and personal care products (PPCPs) from wastewater: a review. *J Environ Manag* 182:620–640
- Wang JL, Wang SZ (2018a) Activation of persulfate (PS) and peroxymonosulfate (PMS) and application for the degradation of emerging contaminants. *Chem Eng J* 334:1502–1517
- Wang JL, Wang SZ (2018b) Microbial degradation of sulfamethoxazole in the environment. *Appl Microbiol Biotechnol* 102:3573–3582
- Wang JL, Zhuan R, Chu LB (2019) The occurrence, distribution and degradation of antibiotics by ionizing radiation: an overview. *Sci Total Environ* 646:1385–1397
- Wang JL, Zhuang ST (2017) Removal of various pollutants from water and wastewater by modified chitosan adsorbents. *Crit Rev Environ Sci Technol* 47:2331–2386
- Wang JL, Zhuang ST, Liu Y (2018) Metal hexacyanoferrates-based adsorbents for cesium removal. *Coord Chem Rev* 374:430–438
- Xing M, Xu LJ, Wang JL (2016) Mechanism of Co(II) adsorption by zero valent iron/graphene nanocomposite. *J Hazard Mater* 301:286–296
- Xu LJ, Wang JL (2017) The application of graphene-based materials for the removal of heavy metals and radionuclides from water and wastewater. *Crit Rev Environ Sci Technol* 47:1042–1105
- Yang WB, Zheng FF, Xue XX, Lu YP (2011) Investigation into adsorption mechanisms of sulfonamides onto porous adsorbents. *J Colloid Interface Sci* 362:503–509
- Zhang C, Lai C, Zeng GM, Huang DL, Yang CP, Wang Y, Zhou YY, Cheng M (2016) Efficacy of carbonaceous nanocomposites for sorbing ionizable antibiotic sulfamethazine from aqueous solution. *Water Res* 95:103–112
- Zhao WT, Guo Y, Lu SG, Yan PP, Sui Q (2016) Recent advances in pharmaceuticals and personal care products in the surface water and sediments in China. *Front Environ Sci Eng* 10(6). <https://doi.org/10.1007/s11783-016-0868-4>
- Zhu X, Wang JL (2017) Comparison of sulfamethazine adsorption by multi-walled carbon nanotubes (MWCNTS) and magnetic MWCNTS from aqueous solution. *Fresenius Environ Bull* 26: 579–589
- Zhuang ST, Cheng R, Kang M, Wang JL (2018) Kinetic and equilibrium of U(VI) adsorption onto magnetic amidoxime-functionalized chitosan beads. *J Clean Prod* 188:655–661
- Zhuang ST, Yin YN, Wang JL (2017) Removal of cobalt ions from aqueous solution using chitosan grafted with maleic acid by gamma radiation. *Nucl Eng Technol* 50:211–215